Materials Science-Poland, *Vol. 27*, *No. 2*, *2009*

Slip casting process for the manufacture of tubular alumina microfiltration membranes

C. FALAMAKI[1,2*], M. BEYHAGHI[1]

[1]Ceramics Department, Materials and Energy Research Center, P.O. Box 14155-4777, Tehran, Iran

[2]Chemical Engineering Department, Amirkabir University of Technology, P.O. Box 15875-4413, Tehran, Iran

A thorough investigation of the slip casting process for the manufacture of tubular alumina microfiltration membranes is presented. For this means an initial powder of an average particle size of 2 μm and broad size distribution (up to 10 μm) for imparting initial large pores during the slip casting process was used. The dispersing ability of sodium carboxymethylcellulose (Na-CMC) and Tiron ($C_6H_4O_8S_2Na_2 \cdot H_2O$) for slips containing 40, 50 and 60 wt. % of alumina was studied. It was shown that Na-CMC is not able to act as a proper dispersant. The kinetics of the slip casting process and time dependences of cast two-dimensional profile were investigated in function of slip concentration. The effect of sintering temperature on the pore microstructure of the final products was investigated. In all cases, the cross sections of the tubular membranes consisted of two regions: an inner thick section, consisting of relatively large pores, and a thin outer section, consisting of smaller pores. This phenomenon was attributed to Na-CMC migration during drying prior to sintering. The ratio of the thicknesses of the two sections depended on the slip concentration and sintering temperature. The average permeable pore size, based on dry nitrogen permeability experiments, was in the range of 0.13–0.24 μm. The controlled use of partial binder migration during cast drying for the production of graded microfilter membranes was addressed.

Key words: *slip casting; alumina; membrane; Na-CMC; Tiron*

1. Introduction

Ceramic membranes have attracted increasing interest in academic and industrial sectors during the last two decades. Most scientific reports concerning ceramic membrane processing discuss flat membrane preparation and far fewer have reported on the manufacture of tubular membranes. The latter include extrusion [1, 2] and centrifugal casting methods [3, 4]. Slip casting is a conventional ceramic processing method, widely used for the production of dense alumina tubular sintered bodies, mostly tradi-

*Corresponding author, e-mail: c.falamaki@aut.ac.ir

tional ceramics [5]. However, there has been no reported research on the application of the latter method to the manufacture of microfilter membranes. This is while slip casting is considered a relatively simple and economical industrial processing route for the production of ceramic bodies and is applied to the manufacture of tubular microfilter membranes by the industrial sector. The present investigation discloses for the first time a systematic approach to study the slip casting process for the manufacture of alumina tubular microfilters.

In conventional alumina slip casting, submicron powder is usually used [5, 6]. This is for guaranteeing slip stability during casting (avoiding particle sedimentation and flocculation). Slip cast bodies obtained by such powders generally result in low permeability of the sintered final products. Using larger particle sizes enhances permeability by introducing initial larger pores. In order to investigate this more comprehensively, the initial powder used in this study consisted of a wide range of particle sizes, from submicron to ten microns with an average around 2 μm.

In this work, high purity alumina sintered microfilters were considered. Sodium carboxymethylcellulose (Na-CMC) was used as dispersant in the first attempt. This was performed according to the existing reports claiming the effectiveness of Na-CMC in slip casting of high purity alumina, acting as a deflocculant, binder and fluxing agent with low residual sodium upon burnout, albeit for sub-micron powders [7, 8]. The sedimentation, zeta potential and rheological behaviour of the slips in function of Na-CMC content and solid loading for the powder used in this work are presented in the first part. Furthermore, the effect of adding a polyvalent organic salt (Tiron, $C_6H_4O_8S_2Na_2 \cdot H_2O$) for improving significantly the slip stability was investigated. This is while existing reports on alumina slips sedimentation behaviour have considered only the effect of one additive as a dispersant [9–14]. To the best of the authors knowledge, few reports have been published concerning the stabilization of alumina slips and which consider both the dispersant as well as the binder [15]. Slip casting was performed on slips containing both Tiron (as a dispersant) and Na-CMC (as a binder and a fluxing agent). The effect of slip solid loading on the slip casting process (two-dimensional cast profile in function of time and slip solid loading) is presented in the second part of this study. In the third part, the effect of slip concentration and sintering temperature on the characteristics of the final sintered microfilter membranes (microstructure, porosity, nitrogen permeability, effective permeable pore size) were investigated.

Finally, the controlled use of partial binder migration during cast drying for the production of graded microfilter membranes was addressed.

2. Experimental

A Martoxide alumina powder (MR42, 99.8 wt. % of α-alumina) was used. The average particle diameter was 2 μm. The particle size distribution was as follows: $0.3 < d_{10} < 0.6$ μm, $1.5 < d_{50} < 2.5$ μm and $3.0 < d_{90} < 5.0$ μm. The specific surface

area was 2.5 $m^2 \cdot g^{-1}$. The impurities were as follows: $Na_2O \leq 0.10$, $CaO \leq 0.05$, $Fe_2O_3 \leq 0.04$ and $SiO_2 \leq 0.06$ wt. %. Na-CMC from Merck was used for several purposes (dispersant, binder, sintering aid). It had the viscosity of around 75 Pa·s at 25 °C when dissolved in distilled water to get a 2 wt. % aqueous solution. Tiron from Acros Co. was used as a dispersant.

Slips containing 40, 50 and 60 wt. % of alumina with Na-CMC alone (N slips) or Na-CMC and Tiron (TN slips) were prepared according to the following procedure: For the N slips, first appropriate quantities of alumina in distilled water were milled in a fast mill for 15 min (first step). Afterwards, appropriate quantities of Na-CMC as aqueous solution (1 wt. %) were added and the resulting mixture was fast milled for 5 min. For the TN slips, Tiron was also added in the first step as 0.0017 g per 1 g of alumina powder. The latter optimum proportion was taken according to ref. [16]. Stable slips for the slip casting processes were produced using a Na-CMC content of 0.05 g per 100 g of alumina for the 40 and 60 wt. % of alumina concentrations.

Sedimentation tests were performed using test tubes filled with 10 cm^3 of the slips. The height of the sediment after 24 h was measured for each case. All the sediment tests were repeated after a time interval of more than 2 months, to ensure that the observed results were not affected by gross errors. The data presented further in the text are the average results.

For the production of tubular green compacts by slip casting, appropriate molds (hydrated calcium sulfate) were prepared. An Iranian plaster of Paris (industrial grade, > 95 wt. % α-hemihydrate calcium sulfate) was used. The ratio of water to plaster of Paris was chosen to be 3/4. After they had formed, the molds were dried for 3 days at 47 °C. The internal diameter of the tubular void was 50 mm.

The slip casting process was performed as follows: the mold was initially filled with the slip (TN slips). As the air-slip interface fell under 5 mm, the mold was gently filled with distilled water. Water was added to avoid crack creation of the upper sections which otherwise were not in contact with the slip. The bottom of the mold was made impermeable by installing a PTFE disk. The slip casting process duration was between 1 and 70 min. The cast compacts were taken out of the mold after 24 h and dried at room temperature for 48 h. Afterwards, they were dried at 70 °C in an oven for 1 h and consecutively put into an electric furnace for sintering. The heating rate applied was 10 °C min^{-1} and the soaking time was 2 h. The sintered samples were fabricated from green compacts with slip casting times of 20 and 5 min for the slips of concentrations 40, 50 and 60 wt. %, respectively. The sintering temperatures were 1375, 1400 and 1450 °C, respectively.

The density of the sintered product was measured according to ASTM C-373-88 (Archimedes' principle). The densities of the dried cast compacts were also measured. As it was not possible to apply the above standard test (because dried casts disintegrated in contact with water), a special method was applied. The dry weight of several segments of the dried cast was measured. Then, the latter were covered gently with a thin layer of vacuum grease, and the weight of the added grease was measured. In

the last step, the surface coated segment weights of the submerged segments were measured. From the above data, the buoyancy force due to the volume of water displaced could be evaluated and corresponded to the total volume of the segment. As a result, the density and porosity of the initial dry cast segments could be readily calculated.

Microstructure evaluation was performed using an XL30 (Philips) instrument. XRD diffraction patterns were taken using a PW3710 (Philips) instrument. Dry N_2 gas permeability measurements were performed using a patented setup [17] in accordance with the ASTM F 316 standard. Circular segments with an approximate projected radius of 10 mm were cut out of the sintered tubular membrane supports. The effective permeable pore diameter was calculated from the permeability measurements for the Knudsen and Poiseuille flow regimes. The mathematical details may be found elsewhere [16]. Zeta-potential measurements were performed using a Malvern zeta sizer 3000 HAS instrument. Rheological measurements (duplicate) were performed using a Brookfield DV III apparatus. Surface porosity was evaluated using Oracle 2 software through analysis of the SEM pictures.

3. Results and discussion

3.1. Slip characterization

The sedimentation heights of the slips containing Na-CMC (N slips) in function of the slip alumina concentration and the quantity of additive added are shown in Fig. 1. As the amount of solid content was different for the test tubes filled with 10 cm^3 of the 40, 50 and 60 wt. % slips, the heights have been normalized for a constant mass of alumina equal to 8.672 g (corresponding to the solid content of the test tube filled with the 40 wt. % slip). The first interesting observation is that by increasing the slip concentration, the packing of the sediment improves. Considering the right hand asymptotes at high CMC concentrations, it is observed that the sediment height of the 60 wt. % slip decreases by ca. 30 % with respect to the 40 wt. % slip. The better particle arrangement at high solids loading is attributed to an intensified steric effect. At high slip solid concentrations, the particles collide more frequently into each other and fewer hydrated layers around each particle are expected [18]. In such circumstances, organic layers of Na-CMC induce a steric effect, eventually acting as a lubricant, preventing particle adhesion due to van der Waals forces.

The second remarkable observation, based on Fig. 1 is that there exists a distinct minimum in the dependence of the height on Na-CMC concentration at each slip concentration. Referring to Fig. 2, it is observed that for the 60 wt. % of alumina slip, viscosity steadily increases with the increase in Na-CMC content in the range of 0.0167 to 0.025 g/100 g of alumina. It should be stated that the slips did exhibit a shear thinning behaviour. Nonetheless, the ratio shear stress/shear rate was approximately constant in the range of the shear rate 0–200 s^{-1} used in this study.

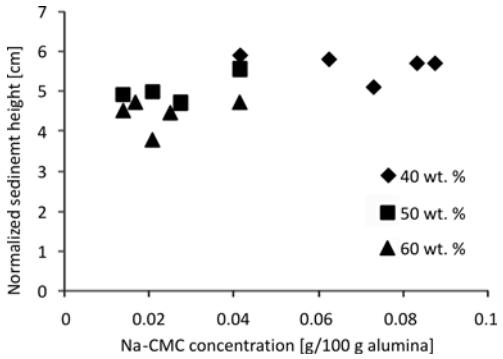

Fig. 1. Sediment height in function of slip and Na-CMC concentration for N slips

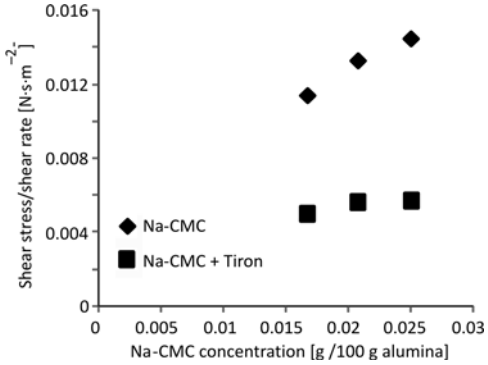

Fig. 2. Shear stress/shear rate in function of Na-CMC content for the N and TN slips

On the other hand, according to Fig. 1, the minimum sediment height (highest packing) corresponds to the Na-CMC content of 0.02075 g/100 g of alumina. Such a behaviour might be explained as follows: if the Na-CMC content lies between 0.0167 to 0.02075 g/100 alumina, more additive is adsorbed on the particles, inferring a higher absolute value of zeta-potential (Fig. 3). More additive does not increase particle charge but, instead, enhances flocculation as a result of bridging effects due to hydrogen bonds [7]. The result is an increase in viscosity, from 0.02075 to 0.025 g Na-CMC/100 alumina content. For 0.0167–0.02075 g Na-CMC/100 g of alumina content, an increase in viscosity is still observed which, at first sight, does not seem to be in concordance with the increase in the zeta-potential observed. This is attributed to the high solid loading of the slip. At high slip concentrations, due to frequent collisions, particles approach each other near their "sphere of influence" [19]. Any increase in the zeta potential in this case results in more interaction (repulsion) between particles, due to a larger sphere of influence. Consequently, any shear stress applied to the slip is accompanied with an increased momentum transfer between particles, due to their strong interaction. Therefore, for concentrated slips, the zeta potential increase may result in an increase in viscosity.

The shift of the minima towards higher values for less concentrated slips, as shown in Fig. 1, may be explained as follows. The amount of Na-CMC added to slip at the minimum for the 60 wt. % slip is 0.02075 g Na-CMC per 100 g of alumina. The corresponding zeta potential is –14.96 mV. For a lower slip concentration, e.g. 50 wt. % of alumina, the minimum sediment height corresponds to 0.0275 g Na-CMC per 100 g of alumina. The corresponding zeta potential was measured to be –36.75 mV. The higher value of the zeta potential at the minimum for the 50 wt. % slip shows that more Na-CMC could be adsorbed on the surface of the alumina particles compared with the 60 wt. % slip. A possible explanation for such a phenomenon is that adsorption of Na-CMC molecules on the surface of alumina particles may be restricted due to steric hindrance at high solid concentrations. In other words, the higher the solid concentra-

tion, the smaller is the amount adsorbed and, as a corollary, the smaller the absolute value of the zeta potential.

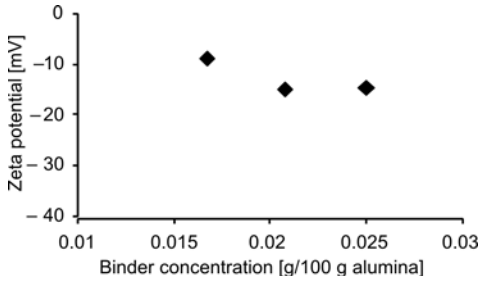

Fig. 3. Zeta potential in function of Na-CMC concentration for the N slips (60 wt. % of alumina slip)

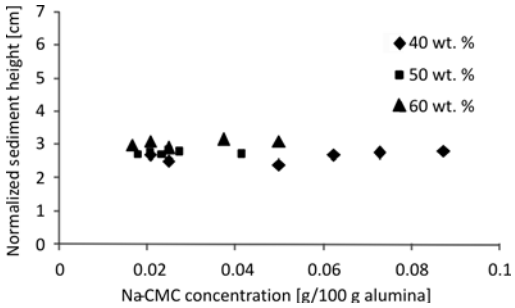

Fig. 4. Sediment height in function of slip and Na-CMC concentration for the TN slips

Although Na-CMC imparted significant dispersion to the slips, the rate of sedimentation in the test tubes was appreciably high (sediment observed after 1 h). It should be recalled that for "membrane support" manufacturing purposes, we have intentionally used an alumina powder with ca. 10 wt. % particles of the diameter in the range 3–5 μm to obtain a porous support of a sufficient high permeability (see ref. [16] for more explanation).To this effect, Tiron was added to the slips before the addition of Na-CMC to try to enhance the slip stability. The sedimentation behaviour is illustrated in Fig. 4. It is observed that Tiron could significantly increase slip stability (the sediment heights being significantly smaller with respect to N slips). It should be noted that any sediment was observable only after 12 h. The authors of the present work do not attribute any specific extremum to the curves in Fig. 4. The zeta-potential of the 60 wt. % slip has a constant value of –31.37±3.21 mV in the Na-CMC concentration range 0.0167–0.025 g/100 g of alumina. The viscosity dependence of the corresponding slips on Na-CMC is shown in Fig. 2. Tiron addition results in a substantial viscosity reduction. Comparing Figs. 4 and 1, it is observed that the trend in slip stability change versus slip alumina concentration has been reversed. The general explanation is the reduction of steric effects in the case of Tiron addition. The particles' surface is totally covered with Tiron and Na-CMC does not appreciably physically adsorb on the Tiron layer. In other words, Na-CMC is present mainly in the aqueous solution and its main effect is to increase the viscosity of the solution (as observed in Fig. 2). Considering the 50 wt. % slip, although the zeta potential is lower than its counterpart for the N slip, the better slip stability is attributed to fewer bridging effects due to the absence of physically adsorbed Na-CMC on the particles.

3.2. Investigation of the slip casting process

Figures 5–7 show the dependences of the tubular cake thickness during slip casting on the sediment height at various slip casting times for the slips containing 40, 50

and 60 wt. % of alumina. The Na-CMC concentration was 0.05 g per 100 g of alumina. Tiron concentration was 0.0017 g per 1 g of alumina.

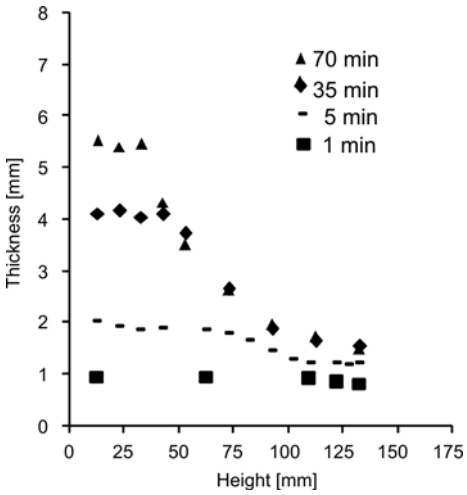

Fig. 5. Thickness in function of height for various slip casting times for the 40 wt. % of alumina slips

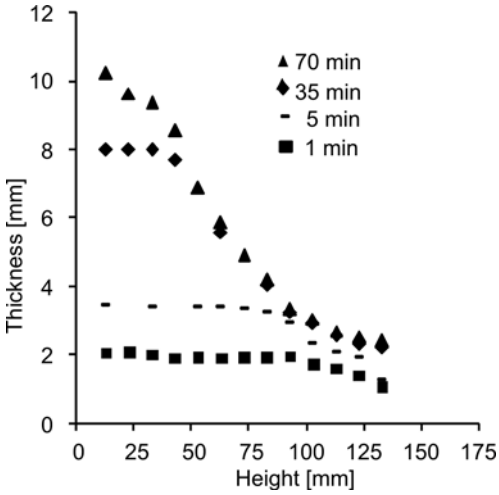

Fig. 6. Thickness in function of height for various slip casting times for the 50 wt. % of alumina slips

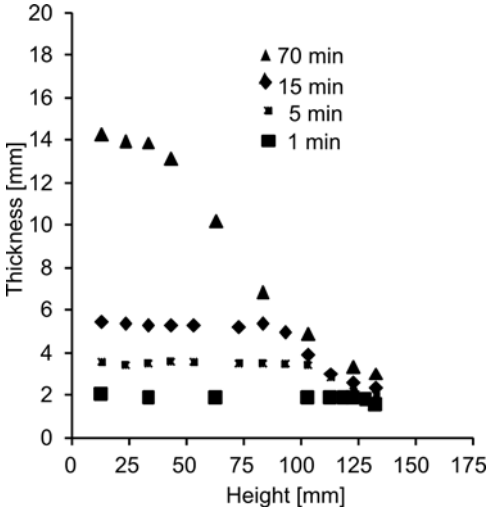

Fig. 7. Thickness in function of height for various slip casting times for the 60 wt. % of alumina slips

A common phenomenon takes place for all the slip concentrations used. At each instant of the slip casting process, the cast may be considered as consisting of two distinct regions: a zone of constant thickness and a zone of variable thickness. By simple visual inspection of the cast after draining the slip, a zone of constant glittering aspect could be observed which corresponds to the constant thickness zone. The reason for the production of such an approximately "constant thickness" cast in the lower

section of the tubular cast may be attributed to the slip sectioning into two distinct zones at all slip casting times: A lower zone of approximately constant concentration and an upper zone of high dilution.

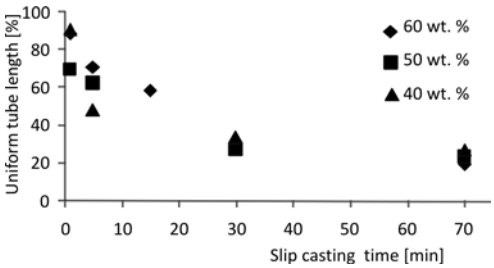

Fig. 8. Uniform tube length in function of slip casting time for various slip concentrations

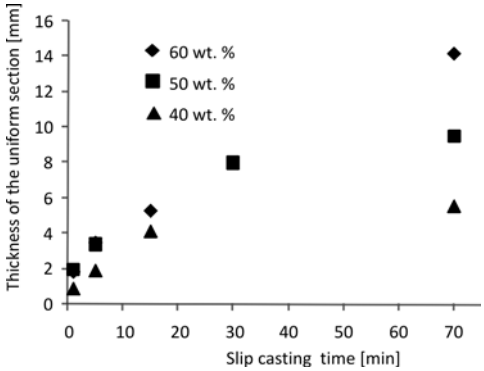

Fig. 9. Uniform tube thickness in function of slip casting time and slip concentration

For all the slip concentrations under consideration, the length of the constant thickness zone decreases with the slip casting time. It should be noted that the length of the constant thickness zone was determined from Figs. 5–7 by finding the point at which the change in the thickness is most abrupt, with respect to the increasing sediment height. Figure 8 shows the uniform tube length in function of the slip casting time for various slip concentrations. It is observed that the rate of length decrease is initially high, and then reduces at longer slip casting periods. The initial period of the decreasing rate decreases with increasing slip concentration. Actually the former rate is approximately constant during most of the slip casting process in the case of 60 wt. % slips.

Figure 9 shows the uniform tube thickness in function of slip casting time and slip concentration. At early times of the casting process, thickness could be correlated with the slip casting time through the following well known equation [20]:

$$L = Kt^{0.5} \tag{1}$$

where L is the thickness [mm], K a constant [mm·min$^{-0.5}$] and t is the time of the slip casting [min]. The value of K depends on the slip initial concentration and has been calculated to be 0.646, 1.148 and 1.195 mm·min$^{-0.5}$ for the 40, 50 and 60 wt. % slip concentrations, respectively.

It is noteworthy to consider the rate of water suction by the mold for each slip concentration used. Slip concentrations of 40 and 50 wt. % of alumina result in approximately similar water suction by the molds (Fig. 10). The reasonable reproducibility of the process for the 40 wt. % of alumina slip may be observed referring to the same figure. A slight discrepancy between the two curves for the 40 wt. % slip is due mainly to the difference of the two molds. Generally, it is impossible to fabricate two identical molds as far as the slip casting behaviour of the molds is concerned. The

60 wt. % slip, on the other hand, results in a significantly reduced rate of water suction. This is attributed to a more packed cast structure for the latter slip concentration.

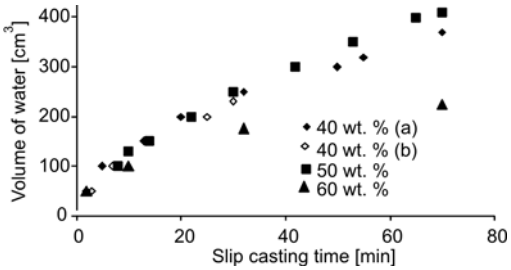

Fig. 10. Amount of water added in function of slip casting time and slip concentration

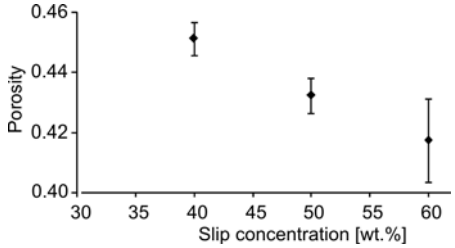

Fig. 11. Porosity of the dried casts in function of slip concentration

Considering Fig. 11, it may be easily observed that the porosity of the dried casts is a function of the slip concentration: the higher the slip concentration, the lower the porosity. The reason for this phenomenon will be explained in the next section.

3.3. Sintered membrane characterization

It should be mentioned that only the "constant thickness" portion of the sintered tubular membranes was investigated. Figures 12a, b show the SEM pictures of the cross section of the inner and outer boundary surfaces of a membrane sintered at 1400° C using a 60 wt. % slip. As far as particle size distribution is concerned no significant difference between the surfaces is observed.

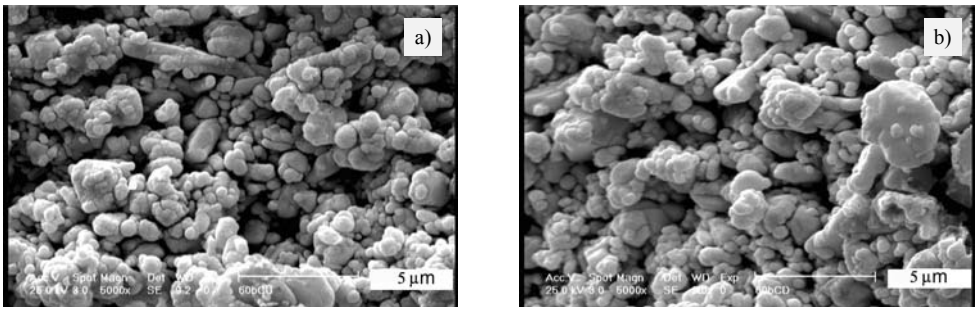

Fig. 12. Cross sections of the inner (left) and outer (right) layers of a sintered sample at 1400 °C using a 60 wt. % slip

The result is the same for the membranes sintered at the same temperature but using different slip concentrations. Generally, no significant particle size gradient exists across the cross section of the membranes. Nonetheless, the outer surfaces consisted of relatively small particles. These surfaces belong to a very thin layer which is the result of small particle migration at the very beginning of the slip casting process. Such

a phenomenon is well known in the processing of ceramics by slip casting [21] and has been referred to as the "clogging effect". The latter phenomenon occurs due to the smaller inertia of smaller particles and a high fluid velocity from the slip towards the mold at the very first stage of the slip casting process. The lower the slip concentration, the greater is the freedom of smaller particles to reach the slip–mold interface. Accordingly, the outer surface of the membrane corresponding to the 40 wt. % slip was observed to have smaller particles in comparison with the particles on the surface of the membrane corresponding to the 60 wt. % slip (Fig. 13).

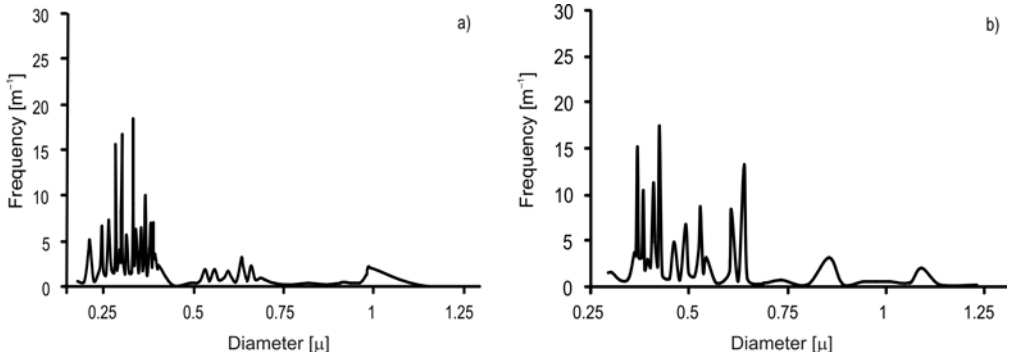

Fig. 13. Outer surface particle size distribution for a sintered membrane using 40 wt. % (a) and 60 wt. % (b) slip at 1400 °C

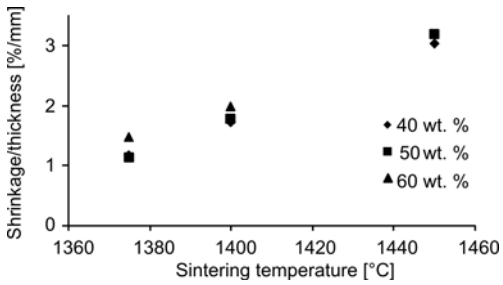

Fig. 14. Ratio of radial shrinkage over thickness for the sintered membranes in function of the sintering temperature and slip concentration

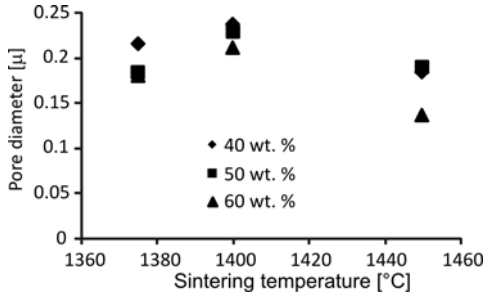

Fig. 15. Average permeable pore diameter of the sintered membranes in function of sintering temperature and slip concentration

Figure 14 shows the ratio of the radial shrinkage to the final thickness of the tubular membranes in function of slip concentration and sintering temperature. Division by the thickness had been performed to cancel out the effect of different initial thicknesses of the slip cast membranes. The values corresponding to the 60 wt. % slip are significantly larger than the values corresponding to the other slip concentrations (the temperature of 1450 °C has been omitted intentionally and will be explained later). The 50 wt. % slip shows a small deviation from the 40 wt. % slip between 1375 °C to 1400 °C. The deviation is even higher at 1450 °C.

Table 1 summarizes the arithmetic average values of porosity of the sintered products for various slip concentrations and sintering temperatures. It is observed that porosity undergoes an abrupt decrease between 1400 °C and 1450 °C. The latter change increases with increasing slip concentration.

Table 1. Average porosity [%] of the sintered products in function of the slip concentration and sintering temperature

Slip concentration [wt. %]	Sintering temperature [°C]		
	1375	1400	1450
40	39	38	30
50	39	40	23
60	40	40	19

The trends presented above may be partially explained referring to Fig. 11. The total length of the error bar at each point corresponds to twice the standard deviation, calculated data obtained from at least 4 experiments. The larger the slip concentration, the higher is the green body density. Increasing the slip concentration from 40 to 60 wt. %, a 6% increase in the raw density is observed. It is the opinion of the authors of this work that the sole 6% difference in the raw density may not cause a 33% difference in density at 1450 °C between the membranes corresponding to 40 and 60 wt. % slips. Sintering behaviour depends upon packing structure, green density, coordination number and particle size distribution [22]. We presume that increasing the slip concentration in the range of 40–60 wt. % of alumina results in a higher homogeneity of the slip during non-agitated slip-casting. In other words, due to more frequent particle collisions at higher slip loadings, a better level of mixing of the particles takes place. This results in a broader particle size distribution throughout the slip and in the cast cake [23]. The enhanced lubricating effect at higher solid loadings, due to less hydrated layers around each particle, also improves particle packing during the slip casting process.

Table 2. Knudsen permeability and slope of the ratio permeability/average pressure drop in the Poiseuille region for the sintered membranes

Sintering temperature [°C]	Slip concentration [wt. %]	Knudsen permeability$\times 10^5$ [$m^3 \cdot s^{-1} \cdot Pa^{-1} \cdot m^{-2}$]	Poiseuille regime slope$\times 10^{11}$ [$m^3 \cdot s^{-1} \cdot Pa^{-2} \cdot m^{-2}$]
1375	40	1.99	4.69
1400	40	1.69	4.36
1450	40	0.83	1.66
1375	50	2.24	4.51
1400	50	1.89	4.64
1450	50	0.98	0.19
1375	60	1.81	3.57
1400	60	1.73	4.01
1450	60	1.59	2.38

The experimental estimates of the Knudsen permeability and slope of the permeability/average pressure drop in the Poiseuille region are summarized in Table 2. The relevant average permeable pore diameters have been calculated and are shown in Fig. 15. For all slip concentrations, an increase in pore the diameter between 1375 °C and 1400 °C and a decrease between 1400 °C and 1450 °C is observed. The 60 wt. % slip results in smaller pores throughout the whole temperature range. Generally, all calculated pore diameters lie in the lower extreme for inorganic microfilter membranes ($0.13 < d < 0.24$ μm). The explanation for this will become apparent in the text below, and upon consideration of some important additional issues which shall now be introduced.

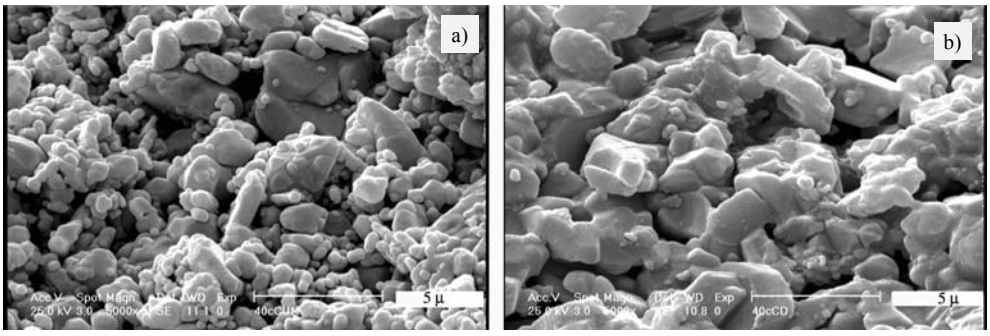

Fig. 16. Micrographs of the middle (left) and inner (right) parts of the cross section of a membrane sintered at 1450 °C using a 40 wt. % slip

As mentioned in the beginning of this section, no appreciable particle size gradient could be observed throughout the entire cross section of the membranes. However, for all the membranes produced, a clear gradient in "pore diameter" across the outer layers could be observed. Figures 16a, b show the micrographs of the middle part and inner layer of the cross section of a membrane sintered at 1450 °C using a 40 wt. % slip. It is clearly observed that the outer layer has undergone appreciable sintering in comparison with the middle layer. SEM analysis of other samples showed that the latter phenomenon is more intense for the membranes produced using higher slip concentrations. The inner and outer surface of a membrane sintered at 1375 °C for a 50 wt. % slip are shown in Fig. 17a, b. It is clearly observed that the outer side has undergone more densification, has smaller pores and also less surface porosity.

All these observations might be explained as follows: The porosity profile across the cross sections of the outermost layers is a result of binder migration during the drying step. The outer surfaces are subject to faster drying. This results in the "concentration" of the dissolved Na-CMC near the outer side of the tubular casts. Actually Na-CMC solidifies near the outer side. As this material is also a sintering aid (it produces active sodium oxide at high temperature), it causes the outer part of the cast to sinter faster. The latter effect is more intense for the casts produced with higher slip solid loadings because, as demonstrated before, higher slip concentrations produce

denser initial casts. Generally, this phenomenon might be of great use in producing graded membranes if used in a controlled manner. The difference in the sintering rate of adjacent layers may result in high stresses between them, especially during the intermediate stages of sintering [16]. In our case, it was observed that the cast pertaining to the 60 wt. % slips underwent longitudinal macrocracks at 1450 °C. This is why the shrinkage of the latter sample was not reported in Fig. 14.

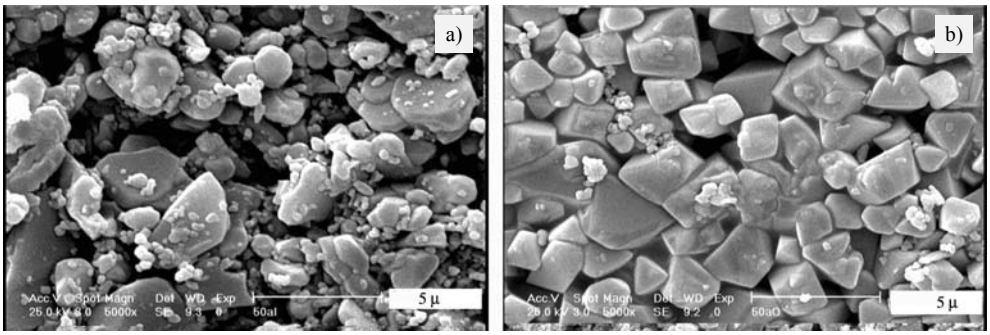

Fig. 17. Inner (left) and outer (right) surfaces of a membrane sintered at 1375 °C using a 50 wt. % slip

The explanations given above elucidate why the calculated microfilter pore diameters are significantly small: they correspond mostly to the denser, outer layers (compare Figs. 17a and b). The thickness of the latter layer for the membranes produced using 40 wt. % slips was approximately 100, 250 and 470 μm at the sintering temperatures 1375, 1400 and 1450 °C, respectively.

Referring again to Fig. 15, it is observed that a clear pore size enlargement occurs in the 1375–1400 °C temperature range. This is attributed to "pore enlargement" of the inner layers during the initial stages of sintering. Initial pore enlargement during the initial sintering stage of alumina green compacts has been reported and discussed in detail by several researchers [24–26]. It is observed that increasing the sintering temperature up to 1450 °C results in a decrease in the pore size, due to significant densification, especially for the outer layers.

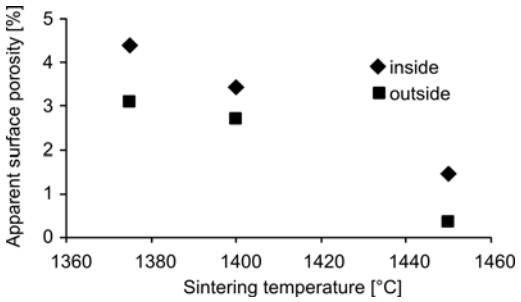

Fig. 18. Apparent surface porosity for the inside and outside surfaces of the sintered membranes fabricated using a 40% slip in function of the sintering temperature

As outlined in the literature (see for example Ref. [16]), the apparent surface porosity is of importance especially if the microfilter is to be coated further for the pro-

duction of ultra- and nanofilters. Therefore, we report the latter parameter for the inside and outside surfaces of the sintered membranes produced using a 40 % slip (Fig. 18). It is observed that the apparent surface porosity decreases approximately linearly as the sintering temperature increases. The outside surface has less porosity with respect to the inner surface at all temperatures.

4. Conclusions

The manufacture of tubular alumina ceramic microfilter membranes by the slip casting method is a rather complicated process. As the final sintered membranes should have reasonable permeability, the average particle size of the initial slip should be larger than that used for conventional slip casting for the production of fully sintered bodies. It was shown in the first part of this work that Na-CMC cannot act as a proper dispersant for stabilizing such alumina slips. The addition of another dispersant, such as Tiron, is indispensable in order to obtain stable slips.

Based on the detailed study performed on the slip casting process, the thickness and two-dimensional profile of the casts, in function of time and slip concentration, are predictable within the ranges of 40-60 wt. % of alumina, and 0–70 min slip casting times.

As far as the membrane characteristics of the final sintered body are concerned, the optimum slip concentration was found to be 40 %. Higher solid loading results in a lower permeability and a smaller effective permeable pore size of the final product. The optimum sintering temperature range is 1375–1400 °C. Within the latter range, the average permeable pore size increases. Higher temperatures result in excessive total and outer layer surface porosity reduction and the creation of macrocracks, especially for high slip concentrations. It is noteworthy to mention that industrial slip casting is generally performed with concentrated slips (typically having a solidity of more than 50 wt. %) in order to minimize water consumption. Therefore, we did not investigate further slips of concentrations lower than 40 wt. %.

In all cases, the cross sections of the tubular membranes consisted of two regions: an inner thick section consisting of relatively large pores and high porosity, and an outer, thin section, consisting of smaller pores and lower porosity. This phenomenon was attributed to binder migration during drying prior to sintering. The ratio of the thicknesses of the two sections depended on the slip concentration and the sintering temperature. The average pore sizes of the membranes were calculated to be within the 0.13–0.24 μm range, and their dependences on the slip concentration and sintering temperature was determined.

Generally, binder migration should be minimized in order to avoid unwanted macrocracks (especially longitudinal) and prematurely high sintering of the outer layers of the cast. The results of our experiments strongly suggest that proper control the “binder migration” phenomenon may be profitably used for the production of functionally graded membranes and is worth further investigation.

References

[1] KHEMAKHEM S., BEN AMAR R., BEN HASSEN R., LARBOT A., BEN SALAH A., COT L., Ind. Ceram., 24 (2004), 207.
[2] ISMAGILOV Z.R., SHKRABINA R.A., KORYABKINA N.A., KIRCHANOV A.A., VERINGA H., PEX P., React. Kinet. Catal. Lett., 60 (1997), 225.
[3] NIJMEIJER A., HUISKES C., SIBELT N.G.M., KRUIDHOF H., VERWEIJ H., Am. Ceram. Soc. Bull. 77 (1998), 95.
[4] KIM K.H., CHO S.J., YOON K.J., KIM J.J., HA J., CHUN D.II, J. Membrane Sci., 199 (2002), 69.
[5] BANNO T., SANO S.and ODA K., , J. Am. Ceram. Soc., 81 (1998), 2933.
[6] CESARINO III J., AKSAY I.A., J. Am. Ceram. Soc., 71 (1988), 1062.
[7] RUYS A.J., SORREL C.C., Am. Ceram. Soc. Bull. 69 (1990), 828.
[8] RUYS A.J., SORRELL C.C., Am. Ceram. Soc. Bull., 75 (1996), 66.
[9] HIDBER P.C., GRAULE T.J., GAUCKLER L.J., J. Eur. Ceram. Soc., 17 (1997), 239.
[10] EVANKO C.R., DZOMBAK D.A., NOVAK J.W.Jr., Coll. Surf. A: Physicochem. Eng. Asp., 110 (1996), 219.
[11] BRISCOE B.J., KHAN A.U., LUCKHAM P.F., J. Eur. Ceram. Soc., 18 (1998), 2141.
[12] SINGH B.P., MENCHAVEZ R., TAKAI C., FUJI M., TAKAHASHI M., J. Coll. Interf. Sci., 291 (2005), 181.
[13] JIANG L., GAO L., Mat. Chem. Phys., 80 (2003), 157.
[14] TSETSEKOU A., AGRATIOTIS C., MILIAS A., J. Eur. Ceram. Soc., 21 (2001), 363.
[15] KHAN A.U., BRISCOE B.J., LUCKHAM P.F., Coll. Surf. A: Phys. Eng. Asp., 161 (2000), 243.
[16] FALAMAKI C., VEYSIZADEH J., J. Membrane Sci., 280 (2006), 899.
[17] FALAMAKI C., AGHAIE A.and ARDESTANI N.R., J. Eur. Ceram. Soc., 21 (2001), 2267.
[18] TARI G., FERREIRA J.M., LYCKFELDT O., J. Eur. Ceram. Soc., 18 (1998), 479.
[19] RICHARDSON D.W., *Modern Ceramic Engineering: Properties, Processing, and Use in Design*, Marcel Dekker, New York, 1992, p. 447.
[20] FALAMAKI C., NAIMI M., AGHAIE A., J. Eur. Ceram. Soc., 26 (2006), 949.
[21] FERREIRA J.M., J. Eur. Ceram. Soc., 18 (1998), 1161.
[22] LINIGER E.G., RAJ R., J. Am. Ceram. Soc., 71 (1988), C-408.
[23] IGA T., J. Ceram. Soc. Japan, 104 (1996), 1143.
[24] FALAMAKI C., AFARANI M.S., AGHAIE A., J. Eur. Ceram. Soc., 24 (2004), 2285.
[25] ZHENG J.and REED J.S., J. Am. Ceram. Soc., 72 (1989), 810.
[26] WHITTEMORE O.J., SIPE J.J., Powder Techn., 9 (1974), 159.

Received 18 May 2008
Revised 21 January 2009